Effects of landscape modification on coastal sediment nitrogen availability, microbial functional gene abundances and N_2O production potential across the tropical-subtropical gradient

Ping Yang[a,b,c,d*], Kam W. Tang[e], Linhai Zhang[a,b], Xiao Lin[a,b,c], Hong Yang[f,g], Chuan Tong[a,b,d*], Yan Hong[a], Lishan Tan[h], Derrick Y. F. Lai[h*], Yalan Tian[a], Wanyi Zhu[a], Manjing Ruan[a], Yongxin Lin[a,b,c*]

[a]*School of Geographical Sciences, Fujian Normal University, Fuzhou 350117, P.R. China*

[b]*Institute of Geography, Fujian Normal University, Fuzhou 350117, P.R. China*

[c]*Fujian Provincial Key Laboratory for Subtropical Resources and Environment, Fujian Normal University, Fuzhou 350117, P.R. China*

[d]*Key Laboratory of Humid Subtropical Eco-geographical Process of Ministry of Education, Fujian Normal University, Fuzhou 350117, P.R. China*

[e]*Department of Biosciences, Swansea University, Swansea SA2 8PP, U. K.*

[f]*College of Environmental Science and Engineering, Fujian Normal University, Fuzhou, 350007, China*

[g]*Department of Geography and Environmental Science, University of Reading, Reading, RG6 6AB, UK*

[h]*Department of Geography and Resource Management, The Chinese University of Hong Kong, Shatin, New Territories, Hong Kong SAR, China*

***Correspondence to:**

Ping Yang (yangping528@sina.cn); Chuan Tong (tongch@fjnu.edu.cn); Derrick Y. F. Lai (dyflai@cuhk.edu.hk); Yongxin Lin (yxlin@fjnu.edu.cn)

Telephone: 086-0591-87445659 **Fax:** 086-0591-83465397

ABSTRACT

Wetland sediment is an important nitrogen pool and a source of the greenhouse gas nitrous oxide (N_2O). Modification of coastal wetland landscape due to plant invasion and aquaculture activities may drastically change this N pool and the related dynamics of N_2O. This study measured the sediment properties, N_2O production and relevant functional gene abundances in 21 coastal wetlands across five provinces along the tropical-subtropical gradient in China, which all had experienced the same sequence of habitat transformation from native mudflats (MFs) to invasive *Spartina alterniflora* marshes (SAs) and subsequently to aquaculture ponds (APs). Our results showed that change from MFs to SAs increased the availability of NH_4^+-N and NO_3^--N and the abundance of functional genes related to N_2O production (*amoA*, *nirK*, *nosZ* I, and *nosZ* II), whereas conversion of SAs to APs resulted in the opposite changes. Invasion of MFs by *S. alterniflora* increased N_2O production potential by 127.9%, whereas converting SAs to APs decreased it by 30.4%. Based on structural equation modelling, nitrogen substrate availability and abundance of ammonia oxidizers were the key factors driving the change in sediment N_2O production potential in these wetlands. This study revealed the main effect patterns of habitat modification on sediment biogeochemistry and N_2O production across a broad geographical and climate gradient. These findings will help large-scale mapping and assessing landscape change effects on sediment properties and greenhouse gas emissions along the coast.

***Keywords*:** Coastal wetland; Habitat change; Nitrogen remineralization; Nitrogen substrates; N_2O production potential; Ammonia oxidation

1. Introduction

The atmospheric concentration of the powerful greenhouse gas nitrous oxide (N_2O) has increased by 123% since the beginning of the industrial era, reaching 333.2 ppbv in 2020 (World Meteorological Organization, 2021). A major source of terrestrial N_2O is microbial transformation of nitrogen (IPCC, 2019) via both nitrification and denitrification (Butterbach-Bahl et al., 2013; Gao et al., 2021; Toyoda et al., 2011; Wu et al., 2019). Quantifying the nitrogen substrate pool, the relevant microbial communities and their activities would be key to understanding N_2O dynamics globally.

Despite covering just 8% of the global land area, wetlands represent one of the world's largest terrestrial nitrogen inventories (Batjes et al., 1996; Xu et al., 2020). Coastal wetlands are particularly important for nitrogen storage (Batjes, 1996; Yang et al., 2016) owing to their high rates of sedimentation and organic matter burial (Chmura et al., 2003; He et al., 2021). Unfortunately, coastal wetlands are increasingly subject to habitat degradation and modification due to land-use change and exotic plant invasion (Murray et al., 2019; Sun et al., 2015; Walker and Smith, 1997), which would likely alter the sediment properties and related microbial production of greenhouse gases such as N_2O (Bahram et al., 2022; Tan et al., 2022; Tian et al., 2020).

There is a total of 5.79×10^6 ha of coastal wetlands along the southern and eastern seaboards of mainland China, accounting for about 10% of the total natural wetlands in the country (Sun et al., 2015). There have been small-scale studies on the effects of habitat change (e.g., plant invasion, agroforestry reclamations, aquaculture reclamation,

68 etc.) on nitrogen mineralization and N_2O emissions in these coastal wetlands (Gao et al.,
69 2019a, 2019b; He et al., 2021; Tan et al., 2020; Yang et al., 2016; Yang et al., 2017;
70 Zhang et al., 2016). In the recent decades, many coastal areas in China have undergone
71 similar sequence of landscape change, with mudflats transformed by the invasion of the
72 exotic cordgrass *Spartina alterniflora* and subsequent clearing of the marsh to construct
73 aquaculture ponds (Duan et al., 2020; Sun et al., 2015; Ren et al., 2019). This provides
74 an opportunity to examine the general pattern of landscape modification effects on
75 sediment properties and N_2O production across the broad geographical range.

76 Ideally, a proper assessment of the landscape change effects would require
77 comparing the habitat characteristics and N_2O production before and after modification.
78 However, such time-lapsed study is not possible because many of the impacted coastal
79 areas in China lack historical information and routine monitoring. Instead, we took
80 samples from 21 coastal wetlands along a 2500-km long transect across the tropical and
81 subtropical zones. Large areas of these wetlands have undergone the same sequence of
82 transformation, from native non-vegetated mudflats to *S. alterniflora* marshes and
83 subsequently to aquaculture ponds. By analyzing the sediments' physicochemical
84 properties, nitrogen-cycling functional gene abundances and N_2O production potentials
85 in all three habitat types, we were able to derive common effect patterns of habitat
86 modifications on sediment N_2O production, regardless of differences in local climate,
87 habitat age, environmental conditions and aquaculture practices. This knowledge will be
88 essential for assessing landscape change effects on greenhouse gas budget at the

89 regional to national scale.

90 This study hypothesized that the conversion of mudflats to *S. alterniflora* marshes
91 would increase the abundances of nitrogen-cycling functional genes and N_2O production
92 potential in the sediment, thanks to an increased supply of nitrogen substrates by the
93 vegetation. Conversely, this study hypothesized that removal of *S. alterniflora* from
94 aquaculture ponds and routine management of pond sediment would decrease nitrogen
95 substrate supply to the sediment, disrupt the sediment microbial community and lower
96 the N_2O production potential.

97 2. Materials and methods

98 *2.1. Study area and sample collection*

99 Sediment samples were collected at 21 coastal wetland sites across the tropical and
100 subtropical climate zones in southeastern China (20°42′ N to 31°51′ N; 109°11′ E to
101 122°11′ E) (Figure 1). These sites span five provinces, with two sites in Shanghai (SH),
102 six in Zhejiang (ZJ), nine in Fujian (FJ), three in Guangdong (GD) and one in Guangxi
103 (GX) (Figure 1). The annual average temperature varied from 11.0 to 23.0 °C and
104 precipitation from 100 to 220 cm across the five provinces. Coastal wetlands in these
105 five provinces cover an area of 2.58×10^6 ha, accounting for 44.5 % of the total area of
106 coastal wetlands in China (Sun et al., 2015). There was approximately 3.6×10^5 ha of
107 tidal flats along the coastal zone of the five provinces (Jia et al., 2021), representing
108 42.4% of the total areas of tidal flats in China. Many of these coastal wetlands have
109 been impacted by the invasion of *S. alterniflora* and subsequent conversion to

aquaculture ponds. Along these coastal zones, *S. alterniflora* marshes cover an area of 3.34×10^4 ha which account for 61.2% of the total *Spartina* marsh area in China (Liu et al., 2018), whereas the aquaculture ponds cover an area of 5.31×10^5 ha, equivalent to 36.9% of the total aquaculture pond area in the country (Duan et al., 2020).

Field sampling campaigns were carried out in the three habitat types at each of the 21 coastal wetland sites, namely native mudflats (MFs), *S. alterniflora* marshes (SAs) and aquaculture ponds (APs), between December 2019 and January 2020. One surface (top 20 cm) sediment sample from each of the triplicate plots established in each habitat was collected with a steel corer (5 cm internal diameter), for a total of 189 surface sediment samples. All sediment samples were kept at 4 °C until use (Hellman et al., 2019).

2.2. Determination of sediment physicochemical properties

In the laboratory, each sediment sample was sifted through a 2-mm sieve before the analysis of various physicochemical parameters. Sediment pH and salinity were measured with a pH meter (Orion 868, USA; a 1:2.5 v/v sediment-deionized water mixture) and a salinity meter (Salt6, Eutech Instruments, USA; a 1:5 v/v sediment-deionized water mixture), respectively. Sediment particle size was measured with a laser particle size analyzer (Master Sizer 2000, Malvern Scientific Instruments, Suffolk, UK). Sediment NO_3^--N and NH_4^+-N were extracted with 2 M KCl solution (Gao et al., 2019b; Yin et al., 2017) and the concentrations of NO_3^--N and NH_4^+-N in the extracts were measured with a flow injection analyzer (Skalar Analytical SAN^{++},

Netherlands). Sediment microbial biomass nitrogen (MBN) content was determined by the fumigation-extraction method (Templer et al., 2003). The concentrations of SO_4^{2-} and Cl^- in sediments were measured with an ion chromatograph (Dionex 2100, USA) following the methods of Chen and Sun (2020).

2.3. DNA extraction and real-time quantitative PCR

Genomic DNA was extracted from each 0.5 g of freeze-dried sediment using FastDNA Spin Kit for Soil (MP Biomedicals, CA, USA) according to the manufacturer's protocol. The quality and quantity of extracted DNA was verified by gel electrophoresis and spectrophotometry (NanoDrop Technologies, Wilmington, USA).

Quantification of nitrogen-cycling functional genes was performed using a real-time polymerase chain reaction (PCR) detection system (CFX384, Bio-Rad Laboratories Inc., Hercules, CA, USA). Each reaction mixture (10 μL) contained 5 μL SYBR mix, an optimized concentration of forward and reverse primers, 1 μL of template (containing approximately 1−10 ng of DNA) and sterilized distilled water. Three negative controls with sterilized distilled water instead of DNA templates were included in the analysis. Nitrogen-cycling functional genes involved in ammonia oxidation (ammonia-oxidizing archaea (AOA) *amoA* and ammonia-oxidizing bacteria (AOB) *amoA*) and denitrification (*nirK*, *nirS*, *nosZ* I, and *nosZ* II) were determined and the details of primers and thermal cycling conditions for PCR are shown in Table S1. The specificity of PCR amplification was assessed by gel electrophoresis and melt curves. Standard curves were generated from a tenfold serial dilution of plasmid DNA containing the target genes. The reaction

efficiency ranged from 88 to 99% with an R^2 value of 0.991 to 0.998.

2.4. Determination of sediment N_2O production potential

The sediment N_2O production potential was measured by anaerobic slurry incubation (Liu et al., 2019; Wang et al., 2017). While sediment N_2O production involves both oxic (e.g. nitrification) and anoxic processes (e.g. denitrification), the terminal step of the process often occurs in anoxic condition (Hu et al., 2015); therefore, we used anaerobic slurry incubation to estimate the *in situ* N_2O production potential. Approximately 30 g of each wet sediment sample and 30 mL of deoxygenated *in situ* overlying water were added to a 200 mL glass bottle and then flushed with N_2 gas (>99.9999% purity) for 5–8 min to create an anoxic condition. All bottles were then incubated for 48 h at the *in situ* temperature, and headspace gas samples were taken at 0, 24, and 48 h. Prior to gas sampling, each glass bottle was shaken on a rotary shaker at 200 rpm for 0.5 h to drive all the N_2O produced in sediment into the headspace. Subsequently, 5 mL of the headspace gas samples were taken with a syringe and 5 mL of pure N_2 gas was added back to each bottle to maintain the atmospheric pressure. The N_2O concentrations in the collected gas samples were measured on a gas chromatograph (GC-2014, Shimadzu, Japan) equipped with an electron capture detector. N_2O production potential [ng N_2O g^{-1} (dry weight) day^{-1}] was then determined based on the change in cumulative N_2O produced per gram of dry sediment over time (Liu et al., 2019; Wang et al., 2017).

2.5. Statistical analysis

Significant differences in sediment physicochemical properties, nitrogen-cycling functional gene abundances, and N_2O production potential among the three habitats were tested by analysis of variance (ANOVA) using the SPSS version 25.0 (IBM, Armonk, NY, USA). Statistical plots were generated using OriginPro 2021 (OriginLab Corp. USA). Pearson correlation analysis was used to examine the relationships between sediment physicochemical properties, nitrogen-cycling functional genes abundances, and N_2O production potential using the vegan package in R software (Version 4.1.0). Structural equation modelling (SEM) was performed using AMOS 21.0 (Amos Development Corporation, Chicago, IL, USA) to evaluate the direct or indirect relationships between habitat change, sediment physicochemical properties, nitrogen-cycling functional gene abundances and N_2O production potential. *A prior* model was established based on our hypotheses and adjusted to achieve an optimal model fit based on the modification indices in the AMOS software (Bahram et al., 2022). Three commonly used indices were selected to assess the goodness of fit of the model, namely Chi-square test (χ^2), goodness of fit index (GFI) and root mean square error of approximation (RMSEA).

3. Results

3.1. Sediment physico-chemical properties.

Across all 21 wetland sites, sediment NH_4^+-N concentration (mean ± SE) in SAs (24.0 ± 1.3 mg kg^{-1}) was significantly higher than that in APs (16.9 ± 1.0 mg kg^{-1}), which was in turn higher than that in MFs (13.3 ± 0.8 mg kg^{-1}) ($p < 0.01$, Figure 2a).

194 NO_3^--N concentration in SAs (1.8 ± 0.1 mg kg^{-1}) was higher than that in MFs (1.3 ± 0.1
195 mg kg^{-1}) and APs (1.5 ± 0.1 mg kg^{-1}) ($p < 0.01$; Figure 2b). MBN concentration was the
196 highest in SAs (26.6 ± 1.9 mg kg^{-1}), followed by APs (16.8 ± 0.8 mg kg^{-1}) and MFs
197 (12.7 ± 0.7 mg kg^{-1}) ($p < 0.01$; Figure 2c). No significant differences were found in
198 sediment pH, salinity, bulk density and percent clay particles among the three habitat
199 types (Table S2). Mean sediment Cl^- concentration was significantly higher in SAs (40.9
200 mg kg^{-1}) than in MFs (36.8 mg kg^{-1}) and APs (37.8 mg kg^{-1}), while mean sediment SO_4^{2-}
201 concentration was significantly higher in APs (17.5 mg kg^{-1}) than in MFs (8.9 mg kg^{-1})
202 and SAs (9.1 mg kg^{-1}) (Table S2).

203 *3.2. Functional gene abundances*

204 The copy numbers of genes for ammonia oxidation (ammonia-oxidizing archaea
205 (AOA) *amoA* and ammonia-oxidizing bacteria (AOB) *amoA*) and denitrification (*nirK*,
206 *nirS*, *nosZ* I, and *nosZ* II) in the different habitat types are shown in Figure 3. Overall,
207 the mean copy numbers of the AOA *amoA*, AOB *amoA* and *nirK* genes were
208 significantly higher in SAs (5.46×10^6, 2.28×10^7 and 9.89×10^7 copies g^{-1}, respectively)
209 than in both APs (2.96×10^6, 1.49×10^7 and 6.77×10^7 copies g^{-1}, respectively) and MFs
210 (2.74×10^6, 1.34×10^7 and 5.83×10^7 copies g^{-1}, respectively) ($p<0.01$; Figures 3a-3c). The
211 mean copy number of the *nirS* genes was significantly higher in APs (13.38×10^7 copies
212 g^{-1}) than in both SAs (9.45×10^7 copies g^{-1}) and MFs (6.99×10^7 copies g^{-1}) ($p<0.01$;
213 Figures 3d). MFs tended to have fewer copies of both *nosZ* I and *nosZ* II genes
214 (6.57×10^7 and 9.72×10^7 copies g^{-1}, respectively) than the other habitat types ($p<0.005$;

215 Figures 3e-3f).

216 *3.3. Sediment N_2O production potential*

217 The mean sediment N_2O production potential varied considerably between sites,
218 ranging 30.8–176.4 ng g^{-1} d^{-1} in MFs, 30.8–388.4 ng g^{-1} d^{-1} in SAs, and 64.1–327.7 ng
219 g^{-1} d^{-1} in APs (Figure 4a). Across all 21 wetland sites, the mean (± SE) sediment N_2O
220 production potential was the highest in SAs (217.1 ± 13.7 ng g^{-1} d^{-1}), followed by APs
221 (151.1 ± 9.3 ng g^{-1} d^{-1}) and MFs (95.3 ± 9.3 ng g^{-1} d^{-1}) (p<0.01; Figure 4b). Therefore,
222 the conversion of MFs to SAs increased sediment N_2O production potential by 127.9%,
223 while the conversion of SAs to APs decreased N_2O production potential by 30.4%.

224 *3.4. Environmental control of sediment N_2O production potential*

225 The results of Pearson correlation analysis between sediment N_2O production
226 potential and various biotic and abiotic variables are shown in Figure 5. For the
227 conversion of MFs to SAs, sediment N_2O production potential was positively correlated
228 to the abundances of AOA *amoA,* AOB *amoA, nirK*, *nirS* and *nosZ* I (p<0.05), as well as
229 the concentrations of NO_3^--N, NH_4^+-N and MBN (p<0.001), but negatively correlated
230 with sediment pH (p<0.05; Figure 5a). For the conversion of SAs to APs, sediment N_2O
231 production potential was positively correlated to the abundances of AOA *amoA,* AOB
232 *amoA* and *nirK* (p<0.05) and the concentrations of NO_3^--N, NH_4^+-N and MBN
233 (p<0.001), but negatively correlated with sediment pH (p<0.001) and *nosZ* II (p<0.05;
234 Figure 5b). The results of SEM analysis revealed that changes in sediment N_2O
235 production potential were mediated mainly through changes in the concentrations of

236 NH_4^+-N and MBN in both habitat modification scenarios (Figure 6a, b). Overall, the
237 concentrations of nitrogen substrates (NO_3^--N and NH_4^+-N) and microbial biomass
238 (MBN) had the largest standardized positive effects on sediment N_2O production
239 potential (Figures 6c, d). In addition, AOA *amoA* was the most important among all
240 functional genes in affecting sediment N_2O production potential during habitat change.

241 ## 4. Discussion

242 Large swaths of coastal mudflat in China have been transformed into marshes by
243 the invasive *S. alterniflora* (Mao et al., 219). To control the spread of *S. alterniflora* and
244 boost food production, many of these marshes have been subsequently cleared and
245 converted into aquaculture ponds (Duan et al., 2021). These drastic landscape
246 transformations have been shown to alter the sediment organic carbon content, carbon
247 remineralization and carbon GHG production (Yang et al., 2022). The rapid expansion
248 of coastal aquaculture in China also raises the alarm of potential increase in N_2O
249 production and emission, thanks to the increasing use of nitrogenous fertilizer and feeds
250 in the farming process (Hu et al., 2012; Zhou et al., 2021).

251 Previous studies have shown that non-native plant species could increase N_2O
252 emissions from coastal wetlands (Gao et al., 2019a; Gao et al., 2019c), likely by
253 increasing organic input into the sediment (Wang et al., 2019a; Xia et al., 2021), which
254 would promote microbial abundance and nitrogen remineralization. This is supported by
255 our observation of significantly higher sediment MBN, NH_4^+-N and NO_3^--N
256 concentrations in SAs relative to MFs (Figure 2). An earlier meta-analysis has shown

257 that increasing NH_4^+-N availability can promote the growth of both AOA and AOB
258 (Ouyang et al., 2018), which would lead to a higher N_2O production. Our correlation
259 and SEM analyses indeed showed that both AOA *amoA* and AOB *amoA* abundances
260 were positively correlated with sediment NH_4^+-N concentrations (Figure 6), and our
261 incubation experiments also showed a significantly higher N_2O production potential in
262 SAs than MFs (Figure 4). These findings support our first hypothesis that conversion of
263 MFs to SAs enhanced sediment N_2O production potential by increasing the supply of
264 nitrogen substrates for microbial-mediated ammonia oxidation.

265 On the other hand, our data showed that the conversion of SAs to APs decreased
266 sediment N_2O production potential (Figure 4), which supported our second hypothesis.
267 Some previous studies have also shown that conversion of coastal marshes to
268 aquaculture ponds could reduce net N_2O emissions (Yang et al., 2017; Yuan et al., 2019;
269 Tan et al., 2020). This at first glance is counter-intuitive, as the use of fertilizer and feeds
270 in aquaculture is widely expected to increase N_2O production and emission (Hu et al.,
271 2012; Williams and Crutzen, 2010). However, it is necessary to consider that some of
272 the added nitrogen (as fertilizer or feeds) would have been sequestered into the sediment
273 or harvested as biomass. Many of the coastal aquaculture ponds in China are for farming
274 shrimp, which has a relatively high nutrient utilization efficiency and consequently, only
275 a small percentage of the added nitrogen would be lost as N_2O emission (Yang et al.,
276 2021). Meanwhile, the removal of *S. alterniflora* during the construction of aquaculture
277 ponds would have eliminated plant-mediated supply of labile organics to the sediment,

which may partly explain the lower NH_4^+-N and NO_3^--N concentrations in AP sediment (Figure 2). Furthermore, a common aquaculture management practice is to dry out the pond sediment and condition it by adding lime between farming seasons (Yang et al., 2021), which would have disrupted the sediment microbial community and its activity. These likely contributed to the lower sediment MBN and N_2O production potential relative to SAs (Figures 2, 5).

Denitrification is a key process in N_2O dynamics in coastal and estuarine environments (Hou et al., 2015; Su et al., 2021; Su et al., 2022). However, the functional genes for denitrification (i.e., *nirK*, *nirS, nosZ* I and *nosZ* II) were found to have limited influence on sediment N_2O production potential in this study (Figure 6), which might be due to the overall low NO_3^--N concentrations across our study sites (Figure 2) and that complete denitrification may produce N_2 instead of N_2O as the end-product (Ciarlo et al., 2008; Wilcock and Sorrell, 2008; Peralta et al., 2010). In contrast, N_2O production potential was most strongly correlated with the functional genes AOA *amoA* and AOB *amoA* (Figures 5, 6), suggesting that ammonia oxidation was the overall rate-limiting step in N_2O production in these wetland ecosystems. This aligns with the findings of Bahram et al. (2022) that the abundance of AOA is a key factor determining the rate of N_2O emissions from global wetlands. Indeed, ammonia oxidizers can drive N_2O production (Hu et al., 2015) especially when NH_4^+-N is the dominant form of available nitrogen (Lin et al., 2017; Wang et al., 2019b), such as the case in our study where sediment NH_4^+-N concentration was an order of magnitude higher than NO_3^--N across

all sampling sites (Figure 2). It was also not surprising to find that AOA *amoA* was more abundant than AOB *amoA* (Figures 3a, b), since AOA can better cope with stresses, giving them a competitive edge over AOB in hypoxic and hypersaline environment (Valentine, 2007; Sun et al., 2022), including wetlands (Sims et al., 2012; Wang et al., 2020; Lin et al., 2021).

5. Conclusions

This study investigated the effects of coastal habitat modification on sediment N_2O production potential across a broad geographical range in China. Our results suggest that conversion of mudflats to *S. alterniflora* marshes enhanced sediment N_2O production potential by increasing the supply of nitrogen substrates and the functional gene abundance for ammonia oxidation, whereas, contrary to common expectation, the subsequent conversion of *S. alterniflora* marshes to aquaculture ponds reduced sediment N_2O production potential owing to a decrease in nitrogen substrate availability and AOA *amoA* gene abundance. These findings highlight that converting *S. alterniflora* marshes to aquaculture ponds could be an effective strategy to achieve multiple benefits of controlling an invasive species, boosting food production and decreasing sediment GHG emission. More importantly, using data from widely distributed sampling sites, we were able to derive common effect patterns of landscape transformation as the results of plant invasion and aquaculture reclamation across the broad geographical and climate range, from tropical to subtropical zones, regardless of local differences in hydrography, biodiversity, management practices or other variables. These findings will facilitate

follow-on large-scale mapping and assessing landscape change effects on coastal ecosystems and N_2O emissions, for example, by incorporating GIS and remote sensing data. While we measured N_2O production in sediment, the actual emissions to the atmosphere could be further modulated by *in-situ* biological/abiotic factors. Measurements of *in-situ* N_2O emissions from the different habitats in future study, using methods such as flux chambers, will be valuable.

Declaration of competing interest

The authors declare that they have no known competing financial interests or personal relationships that could have appeared to influence the work reported in this paper.

Acknowledgements

This research was supported by the Natural Science Foundation of Fujian Province, China (Grant No. 2020J01136, and 2022R1002006), the National Natural Science Foundation of China (NSFC) (Grant No. 41801070, and No. 41671088), and the Research Grants Council of the Hong Kong Special Administrative Region, China (Project No. CUHK 14122521).

References

Bahram, M., Espenberg, M., Pärn, J., Lehtovirta-Morley, L., Anslan, S., Kasak, K., Kõljalg, U., Liira, J., Maddison, M., Moora, M., Niinemets, Ü., Öpik, M., Pärtel, M., Soosaar, K., Zobel, M., Hildebrand, F., Tedersoo, L., Mander, Ü., 2022. Structure and function of the soil microbiome underlying N_2O emissions from global wetlands. Nat. Commun. 13, 1430. https://doi.org/10.1038/s41467-022-29161-3

342 Batjes, N.H., 1996. Total carbon and nitrogen in the soils of the world. Eur. J. Soil Sci.
343 47, 151–163. https://doi.org/10.1111/ejss.12115
344 Butterbach-Bahl, K., Baggs, E.M., Dannenmann, M., Kiese, R.,
345 Zechmeister-Boltenstern, S., 2013. Nitrous oxide emissions from soils: how well do
346 we understand the processes and their controls? Philos. T. R. Soc. B: Biol. Sci. 368,
347 20130122. https://doi.org/10.1098/rstb.2013.0122
348 Chen, B.B., Sun, Z.G., 2020. Effects of nitrogen enrichment on variations of sulfur in
349 plant-soil system of *Suaeda salsa* in coastal marsh of the Yellow River estuary.
350 China. Ecol. Indic. 109, 105797. https://doi.org/10.1016/j.ecolind.2019.105797
351 Chmura, G.L., Anisfeld, S.C., Cahoon, D.R., Lynch, J.C., 2003. Global carbon
352 sequestration in tidal, saline wetland soils. Global Biogeochem. Cy. 17(4), 1111.
353 https://doi.org/10.1029/2002GB001917
354 Ciarlo, E., Conti, M., Bartoloni, N., Rubio, G., 2008. Soil N_2O emissions and
355 $N_2O/(N_2O+ N_2)$ ratio as affected by different fertilization practices and soil moisture.
356 Biol. Fert. S. 44, 991–995. https://doi.org/10.1007/s00374-008-0302-6
357 Duan, Y.Q., Li, X., Zhang, L.P., Chen, D., Liu, S.A., Ji, H.Y., 2020. Mapping
358 national-scale aquaculture ponds based on the Google Earth Engine in the Chinese
359 coastal zone. Aquaculture 520, 734666.
360 https://doi.org/10.1016/j.aquaculture.2019.734666
361 Duan, Y.Q., Tian, B., Li, X., Liu, D.Y., Sengupta, D., Wang, Y.J., Peng, Y., 2021.
362 Tracking changes in aquaculture ponds on the China coast using 30 years of Landsat
363 images. Int. J. Appl. Earth Obs. 102, 102383. https://doi.
364 org/10.1016/j.jag.2021.102383
365 Gao, D.Z., Hou, L.J., Liu, M., Zheng, Y.L., Yin, G.Y., Niu, Y.H., 2021. N_2O emission
366 dynamics along an intertidal elevation gradient in a subtropical estuary: Importance
367 of N_2O consumption. Environ. Res. 205, 112432.
368 https://doi.org/10.1016/j.envres.2021.112432
369 Gao, G.F., Li, P.F., Zhong, J.X., Shen, Z.J., Chen, J., Li, Y.T., Isabwe, A., Zhu, X.Y.,
370 Ding, Q.S., Zhang, S., Gao, C.H., Zheng, H.L., 2019a. *Spartina alterniflora* invasion
371 alters soil bacterial communities and enhances soil N_2O emissions by stimulating

soil denitrification in mangrove wetland. Sci. Total Environ. 653, 231–240. https://doi.org/10.1016/j.scitotenv.2018.10.277

Gao, D.Z., Liu, M., Hou, L.J., Lai D.Y.F., Wang, W.Q., Li, X.F., Zeng, A.Y., Zheng, Y.L., Han, P., Yang, Y., Yin, G.Y., 2019b. Effects of shrimp-aquaculture reclamation on sediment nitrate dissimilatory reduction processes in a coastal wetland of southeastern China. Environ. Pollut. 255, 113219. https://doi.org/10.1016/j.envpol.2019.113219

Gao, D.Z., Hou, L.J., Li, X.F., Liu, M., Zheng, Y.L., Yin, G.Y., Yang, Y., Liu, C., Han, P., 2019c. Exotic *Spartina alterniflora* invasion alters soil nitrous oxide emission dynamics in a coastal wetland of China. Plant Soil 442, 233-246. https://doi.org/10.1007/s11104-019-04179-7

He, G.S., Wang, K.Y., Zhong, Q.C., Zhang, G.L., van den Bosch, C.K., Wang, J.T., 2021. Agroforestry reclamations decreased the CO_2 budget of a coastal wetland in the Yangtze estuary. Agr. Forest Meteorol. 296, 108212. https://doi.org/10.1016/j.agrformet.2020.108212

Hellman, M., Bonilla-Rosso, G., Widerlund, A., Juhanson, J., Hallin, S., 2019. External carbon addition for enhancing denitrification modifies bacterial community composition and affects CH_4 and N_2O production in sub-arctic mining pond sediments. Water Res. 158, 22–33. https://doi.org/10.1016/j.watres.2019.04.007

Hou, L.J., Yin, G.Y., Liu, M., Zhou, J.L., Zheng, Y.L., Gao, J., Zong, H.B., Yang, Y., Gao, L., Tong, C.F., 2015. Effects of sulfamethazine on denitrification and the associated N_2O release in estuarine and coastal sediments. Environ. Sci. Technol. 49(1), 326–333. https://doi.org/10.1021/es504433r

Hu, H.W., Chen, D., He, J.Z., 2015. Microbial regulation of terrestrial nitrous oxide formation: understanding the biological pathways for prediction of emission rates. FEMS Microbiol. Rev. 39, 729–749. https://doi.org/10.1093/femsre/fuv021

Hu, Z., Lee, J.W., Chandran, K., Kim, S., Khanal, S.K., 2012. Nitrous oxide (N_2O) emission from aquaculture: a review. Environ. Sci. Technol. 46(12), 6470-6480. https://doi. org/10.1021/es300110x

IPCC, 2019. In: Calvo Buendia, E., Tanabe, K., Kranjc, A., Baasansuren, J., Fukuda, M., Ngarize, S. (Eds.), 2019 Refinement to the 2006 IPCC Guidelines for National Greenhouse Gas Inventories, Volum 4. IPCC, Switzerland. Kanagawa, Japan Chapter 07.

Jia, M.M., Wang, Z.M., Mao, D.H., Ren, C.Y., Wang, C., Wang, Y.Q., 2021. Rapid, robust, and automated mapping of tidal flats in China using time series Sentinel-2 images and Google Earth Engine. Remote Sens. Environ. 255, 112285. https://doi.org/10.1016/j.rse.2021.112285

Lin, Y.X., Ding, W.X., Liu, D.Y., He, T.H., Yoo, G., Yuan, J.J., Chen, Z.M., Fan, J.L., 2017. Wheat straw-derived biochar amendment stimulated N_2O emissions from rice paddy soils by regulating the *amoA* genes of ammonia-oxidizing bacteria. Soil Biol. Biochem. 113, 89–98. https://doi.org/10.1016/j.watres.2021.117682

Lin, Y.X., Hu, H.W., Ye, G.P., Fan, J.B., Ding, W.X., He, Z.Y., Zheng, Y., He, J.Z., 2021. Ammonia-oxidizing bacteria play an important role in nitrification of acidic soils: A meta-analysis. Geoderma 404, 115395. https://doi.org/10.1016/j.geoderma.2021.115395

Liu, J.G., Hartmann, S.C., Keppler, F., Lai, D.Y.F., 2019. Simultaneous abiotic production of greenhouse gases (CO_2, CH_4, and N_2O) in Subtropical Soils. J. Geophys. Res.-Biogeo. 124(7), 1977–1987. https://doi.org/10.1029/2019JG005154

Liu, M.Y., Mao, D.H., Wang, Z.M., Li, L., Man, W.D., Jia, M.M., Ren, C.Y., Zhang, Y.Z., 2018. Rapid invasion of *Spartina alterniflora* in the coastal zone of mainland China: new observations from landsat OLI images. Remote Sens. 10, 1933. https://doi.org/10.3390/rs10121933

Mao, D.H., Liu, M.Y., Wang, Z.M., Li, L., Man, W.D., Jia, M.M., Zhang, Y., 2019. Rapid invasion of *Spartina alterniflora* in the coastal zone of mainland China: Spatiotemporal patterns and human prevention. Sensors *19*(10), 2308. https://doi.org/10.3390/s19102308

Murray, N.J., Phinn, S.R., DeWitt, M., Ferrari, R., Johnston, R., Lyons, M.B., Fuller, R.A., 2019. The global distribution and trajectory of tidal flats. Nature 565, 222–225. https://doi.org/10.1038/s41586-018-0805-8

Ouyang, Y., Evans, S.E., Friesen, M.L., Tiemann, L.K., 2018. Effect of nitrogen fertilization on the abundance of nitrogen cycling genes in agricultural soils: A meta-analysis of field studies. Soil Biol. Biochem. 127, 71–78. https://doi.org/10.1016/j.soilbio.2018.08.024

Peralta, A.L., Matthews, J.W., Kent, A.D., 2010. Microbial community structure and denitrification in a wetland mitigation bank. Appl. Environ. Microb. 76, 4207–4215. https://doi.org/10.1128/aem.02977-09

Ren, C.Y., Wang, Z.M., Zhang, Y.Z., Zhang, B., Chen, L., Xia, Y.B., Xiao, X.M., Doughty, R.B., Liu, M.Y., Jia, M., Mao, D.H., Song, K.S., 2019. Rapid expansion of coastal aquaculture ponds in China from Landsat observations during 1984–2016. J. Appl. Earth Obs. 82, 101902. https://doi.org/10.1016/j.jag.2019.101902

Sims, A., Horton, J., Gajaraj, S., McIntosh, S., Miles, R.J., Mueller, R., Reed, R., Hu, Z., 2012. Temporal and spatial distributions of ammonia-oxidizing archaea and bacteria and their ratio as an indicator of oligotrophic conditions in natural wetlands. Water Res. 46, 4121–4129. https://doi.org/10.1016/j.watres.2012.05.007

Su, X.X., Wen, T., Wang, Y.M., Xu, J.S., Cui, L., Zhang, J.B., Xue, X.M., Ding, K., Tang, Y.J., Zhu, Y.G., 2021. Stimulation of N_2O emission via bacterial denitrification driven by acidification in estuarine sediments. Global Change Biol. 27, 5564–5579. https://doi.org/10.1111/gcb.15863

Su, X.X., Yang, L.Y., Yang, K., Tang, Y.J., Wen, T., Wang, Y.M., Rillig, M.C., Rohe, L., Pan, J.L., Li, H., Zhu, Y.G., 2022. Estuarine plastisphere as an overlooked source of N_2O production. Nat. Commun. 13, 3884. https://doi.org/10.1038/s41467-022-31584-x

Sun, X.X., Zhao, J., Zhou, X., Bei, Q.C., Xia, W.W., Zhao, B.Z., Zhang, J.B., Jia, Z.J., 2022. Salt tolerance-based niche differentiation of soil ammonia oxidizers. ISME J. *16*, 412–422. http://dx.doi.org/10.1038/s41396-021-01079-6

Sun, Z.G., Sun, W.G., Tong, C., Zeng, C.S., Yu, X., Mou, X.J., 2015. China's coastal wetlands: Conservation history, implementation efforts, existing issues and strategies for future improvement. Environ. Int. 79, 25–41. http://dx.doi.org/10.1016/j.envint.2015.02.017V

Tian, H.Q., Xu, R.T., Canadell, J.G., Thompson, R.L., Winiwarter, W., Suntharalingam, P., Davidson, E.A., Ciais, P., Jackson, R.B., et al., 2020. A comprehensive quantification of global nitrous oxide sources and sinks. Nature 586, 248–256. https://doi.org/10.1038/s41586-020-2780-0

Tan, L.S., Ge, Z.M., Ji, Y.H., Lai, D.Y.F., Temmerman, S., Li, S.H., Li, X.Z., Tang, J.W., 2022. Land use and land cover changes in coastal and inland wetlands cause soil carbon and nitrogen loss. Global Ecol. Biogeogr. 31(12), 2541–2563. https://doi.org/10.1111/geb.13597

Tan, L.S., Ge, Z.M., Zhou, X.H., Li, S.H, Li, X.Z., Tang, J.W., 2020. Conversion of coastal wetlands, riparian wetlands, and peatlands increases greenhouse gas emissions: A global meta-analysis. Global Change Biol. 26, 1638–1653. http://dx.doi.org/10.1111/gcb.14933

Templer, P., Findlay, S., Lovett, G., 2003. Soil microbial biomass and nitrogen transformations among five tree species of the Catskill Mountains, New York, USA. Soil Biol. Biochem. 35(4), 607–613. http://dx.doi.org/10.1016/s0038-0717(03)00006-3

Toyoda, S., Yano, M., Nishimura, S.I., Akiyama, H., Hayakawa, A., Koba, K., Ogawa, N.O., 2011. Characterization and production and consumption processes of N_2O emitted from temperate agricultural soils determined via isotopomer ratio analysis. Global Biogeochem. Cy. 25, 96–101. https://doi.org/10.1029/2009GB003769

Valentine, D.L., 2007. Adaptations to energy stress dictate the ecology and evolution of the Archaea. Nat. Rev. Microbiol. 5, 316–323. https://doi.org/10.1038/nrmicro1619

Walker, L.R., Smith, S.D., 1992. Impacts of invasive plants on community and ecosystem properties. In: Luken, J.O., Thieret, J.W. (eds) Assessment and management of plant invasion. Spriger-Verlag, New York, pp 69–94.

Wang, C., Tang, S.Y., He, X.J., Ji, G.D., 2020. The abundance and community structure of active ammonia-oxidizing archaea and ammonia-oxidizing bacteria shape their activities and contributions in coastal wetlands. Water Res. 171, 115464. http://dx.doi.org/10.1016/j.watres.2019.115464

Wang, W.Q., Sardans, J., Wang, C., Zeng, C.S., Tong, C., Chen, G., Huang, J.F., Pan, H.R., Peguero, G., Vallicrosa, H., Penuelas, J., 2019a. The response of stocks of C, N, and P to plant invasion in the coastal wetlands of China. Global Change Biol. 25, 733–743. https://doi.org/10.1111/gcb.14491

Wang, L., Li, K., Sheng, R., Li, Z.H., Wei, W.X., 2019b. Remarkable N_2O emissions by draining fallow paddy soil and close link to the ammonium-oxidizing archaea communities. Sci. Rep. 9, 2550. http://dx.doi.org/10.1038/s41598-019-39465-y

Wang, W.Q., Sardans, J., Wang, C., Zeng, C.S., Tong, C., Asensio, D., Peñuelas, J., 2017. Relationships between the potential production of the greenhouse gases CO_2, CH_4 and N_2O and soil concentrations of C, N and P across 26 paddy fields in southeastern China. Atmos. Environ. 164, 458–467. http://dx.doi.org/10.1016/j.atmosenv.2017.06.023

Wilcock, R.J., Sorrell, B.K., 2008. Emissions of greenhouse gases CH_4 and N_2O from low-gradient streams in agriculturally developed catchments. Water, Air, and Soil Pollution 188, 155–170. https://doi.org/10.1029/2017gb005826

Williams, J., Crutzen, P. J., 2010. Nitrous oxide from aquaculture. Nat. Geosci. 3(3), 143-143. https://doi.org/10.1038/ngeo804

World Meteorological Organization, 2021. WMO Greenhouse Gas Bulletin (GHG Bulletin) - No.17: The State of Greenhouse Gases in the Atmosphere Based on Global Observations through 2020. https://library.wmo.int/doc_num.php?explnum_id=10904

Wu, D., Well, R., Cárdenas, L.M., Fuß, R., Lewicka-Szczebak, D., Köster, J.R., Brüggemann, N., Bol, R., 2019. Quantifying N_2O reduction to N_2 during denitrification in soils via isotopic mapping approach: model evaluation and uncertainty analysis. Environ. Res. 179, 108806. https://doi.org/10.1016/j.envres.2019.108806

Xia, S.P., Wang, W.Q., Song, Z.L., Kuzyakov, Y., Guo, L.D., Van Zwieten, L., Li, Q., Hartley, I.P., Yang, Y.H., Wang, Y.D., Quine, T.A., Liu, C.Q., Wang, H.L., 2021. *Spartina alterniflora* invasion controls organic carbon stocks in coastal marsh and

519 mangrove soils across tropics and subtropics. Global Change Biol. 27, 1627–1644.
520 https://doi.org/10.1111/gcb.15516
521 Xu, L., He, N.P., Yu, G.R., 2020. Nitrogen storage in China's terrestrial ecosystems. Sci.
522 Total Environ. 709, 136201. https://doi.org/10.1016/j.scitotenv.2019.136201
523 Yang, P., Bastviken, D., Jin, B.S., Mou, X.J., Tong, C., 2017. Effects of coastal marsh
524 conversion to shrimp aquaculture ponds on CH_4 and N_2O emissions. Estuar. Coast.
525 Shelf S. 199, 125–131. https://doi.org/10.1016/j.ecss.2017.09.023
526 Yang, P., Zhao, G., Tong, C., Tang, K.W., Lai, D.Y.F., Li, L., Tong, C., 2021. Assessing
527 nutrient budgets and environmental impacts of coastal land-based aquaculture
528 system in southeastern China. Agr. Ecosyst. Environ. 322, 107662.
529 https://doi.org/10.1016/j.agee.2021.107662
530 Yang, P., Zhang, L.H., Lai, D.Y.F., Yang, H., Tan, L.S., Luo, L.J., Tong, C., Hong, Y.,
531 Zhu, W.Y., Tang, K.W., 2022. Landscape change affects soil organic carbon
532 mineralization and greenhouse gas production in coastal wetlands. Global
533 Biogeochem. Cy. 36, e2022GB007469. https://doi.org/10.1029/2022GB007469
534 Yang, W., An, S.Q.,Zhao, H., Xu, L.Q., Qiao, Y.J., Cheng, X.L., 2016. Impacts of
535 *Spartina alterniflora* invasion on soil organic carbon and nitrogen pools sizes,
536 stability, and turnover in a coastal salt marsh of eastern China. Ecol. Eng. 86,
537 174–182. http://dx.doi.org/10.1016/j.ecoleng.2015.11.010
538 Yin, G.Y., Hou, L.J., Liu, M., Li, X.F., Zheng, Y.L., Gao, J., Lin, X.B., 2017. DNRA in
539 intertidal sediments of the Yangtze Estuary. J. Geophys. Res.-Biogeo. 122(8),
540 1988–1998. https://doi.org/10.1002/2017JG003766
541 Yuan, J.J., Xiang, J., Liu, D.Y., Kang, H., He, T.H., Kim, S., Lin, Y.X., Freeman, C.,
542 Ding, W.X., 2019. Rapid growth in greenhouse gas emissions from the adoption of
543 industrial-scale aquaculture. Nat. Clim. Change 9(4), 318–322.
544 https://doi.org/10.1038/s41558-019-0425-9
545 Zhang, Y.H., Xu, X.J., Li, Y., Huang, L.D., Xie, X.J., Dong, J.M., Yang, S.Q., 2016.
546 Effects of *Spartina alterniflora* invasion and exogenous nitrogen on soil nitrogen
547 mineralization in the coastal salt marshes. Ecol. Eng. 87, 281–287.
548 http://dx.doi.org/10.1016/j.ecoleng.2015.12.003

549 Zhou, Y., Huang, M., Tian, H.Q., Xu, R.T., Ge, J., Yang, X.G., Liu, R.X., Sun, Y.X.,
550 Pan, S.F., Gao, Q.F., Dong, S.L., 2021. Four decades of nitrous oxide emission from
551 Chinese aquaculture underscores the urgency and opportunity for climate change
552 mitigation. Environ. Res. Lett. 16(11), 114038.
553 https://doi.org/10.1088/1748-9326/ac3177

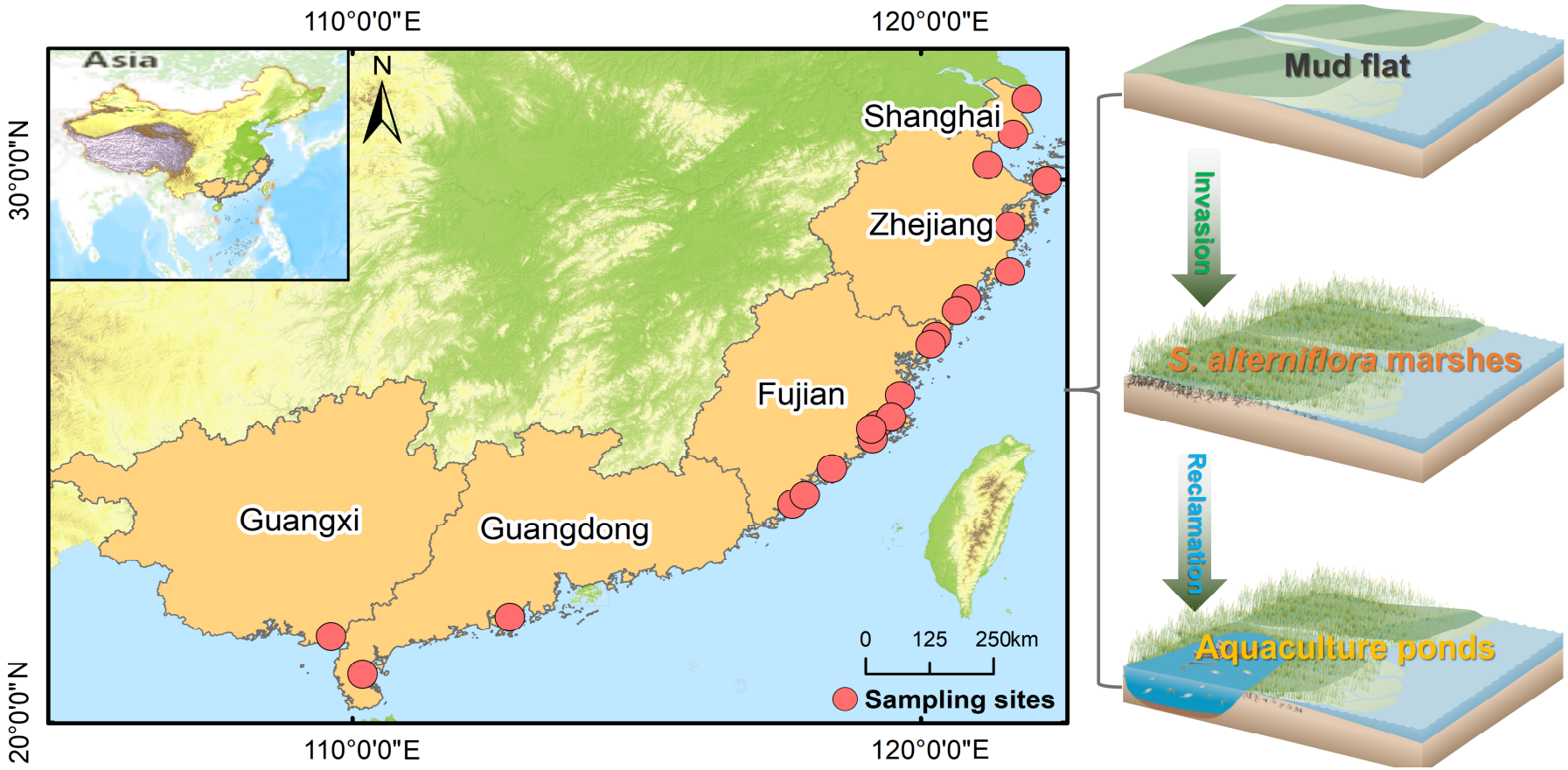

Figure 1. Locations of the 21 coastal wetland sites in southeastern China. At each site, three habitat types were sampled, including mudflats, *Spartina alterniflora* marshes and aquaculture ponds.

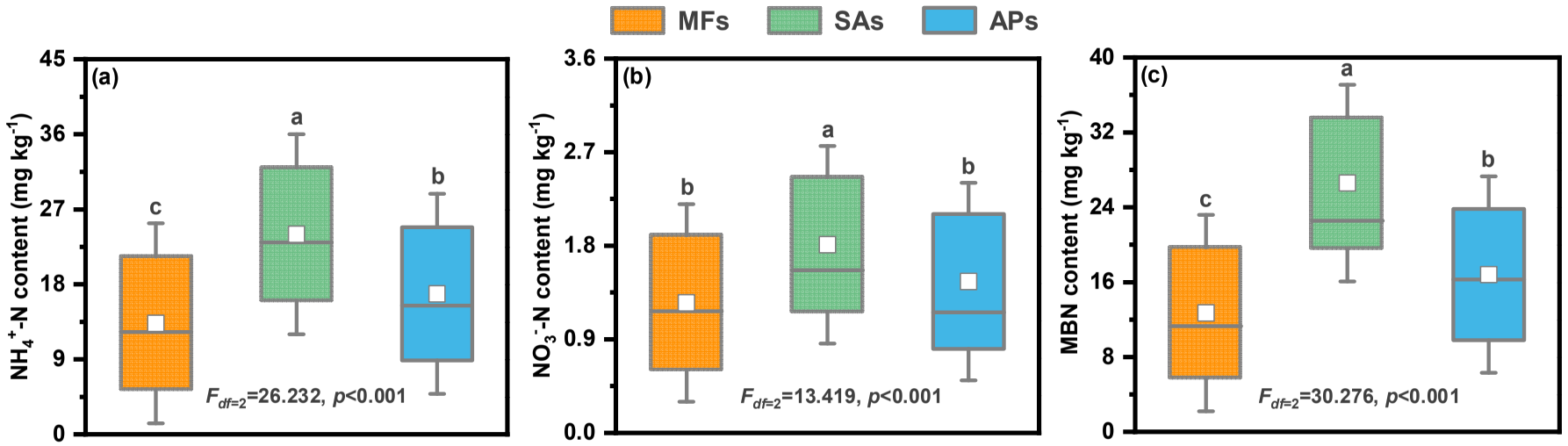

Figure 2. Box plots of nitrogen substrates (NH_4^+-N, NO_3^--N) and microbial biomass nitrogen (MBN) in surface sediment of the three wetland habitat types: mudflats (MFs), *S. alterniflora* marshes (SAs) and aquaculture ponds (APs). [The boxes, center line, and whiskers represent the 25th – 75th percentiles, median value, and 5th and 95th percentiles, respectively.] Different letters above the boxes indicate significant differences between habitat types (p<0.05).

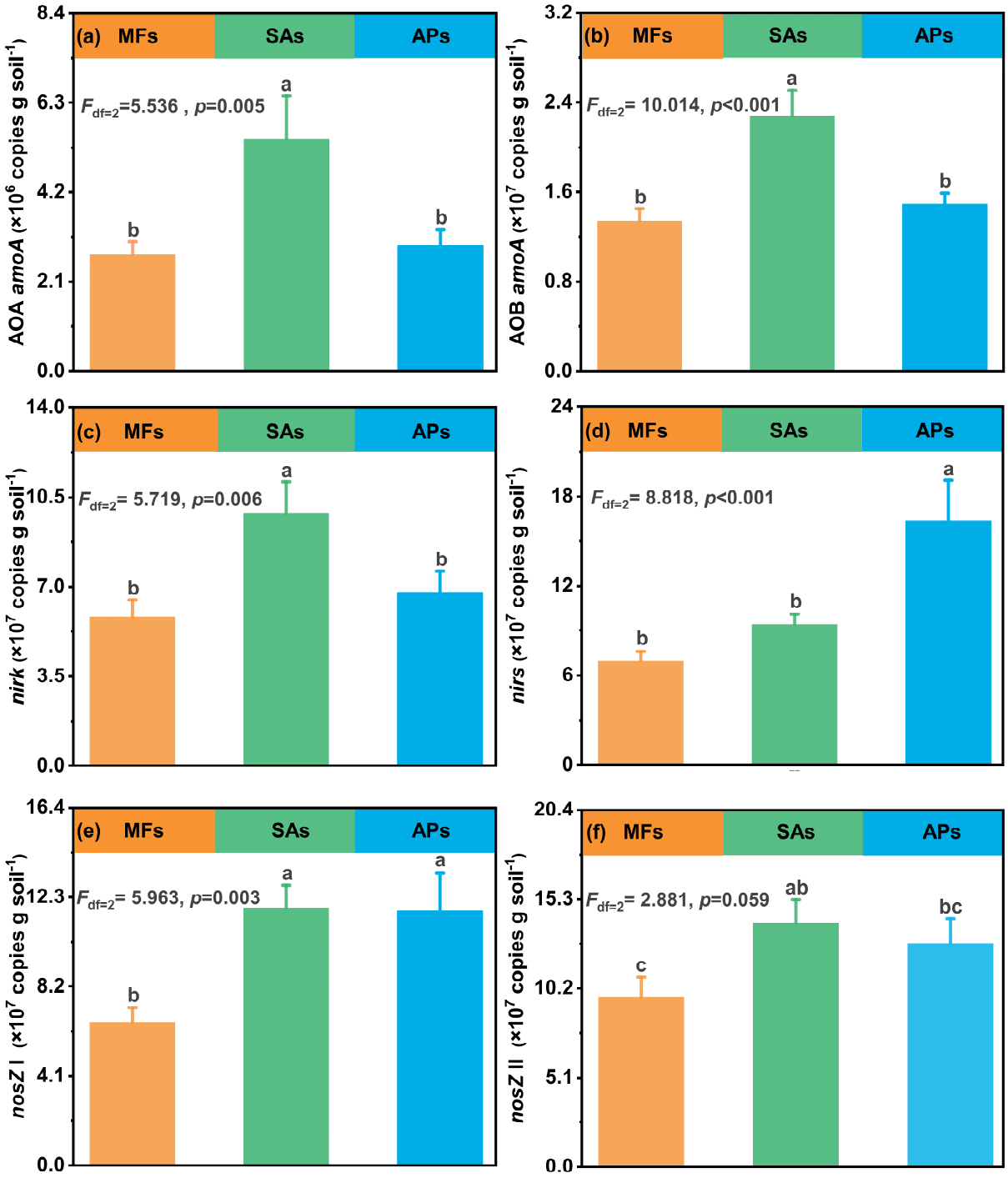

Figure 3. Sediment gene abundances (AOA *amoA*, AOB *amoA*, *nirK*, *nirS*, *nosZ* I and *nosZ* II) in the three habitat types: mudflats (MFs), *S. alterniflora* marshes (SAs) and aquaculture ponds (APs). Bars represent mean ± 1SE (n = 63). Different letters above the bars indicate significant differences ($p < 0.05$) between the habitat types.

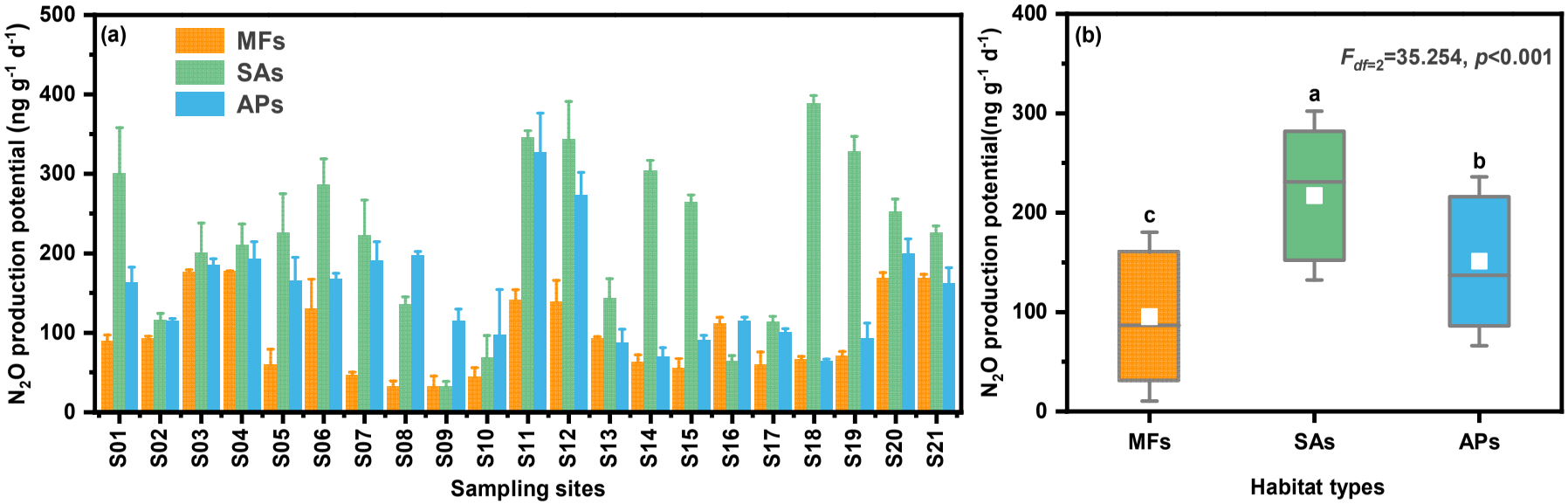

Figure 4. (a) Sediment N_2O production potential in the three habitat types: mudflats (MFs), *S. alterniflora* marshes (SAs) and aquaculture ponds (APs) at each of the wetland sites. (b) Data from all 21 wetland sites combined in box plots to compare sediment N_2O production potentials between habitat types; different letters above the boxes indicate significant differences (p<0.05).

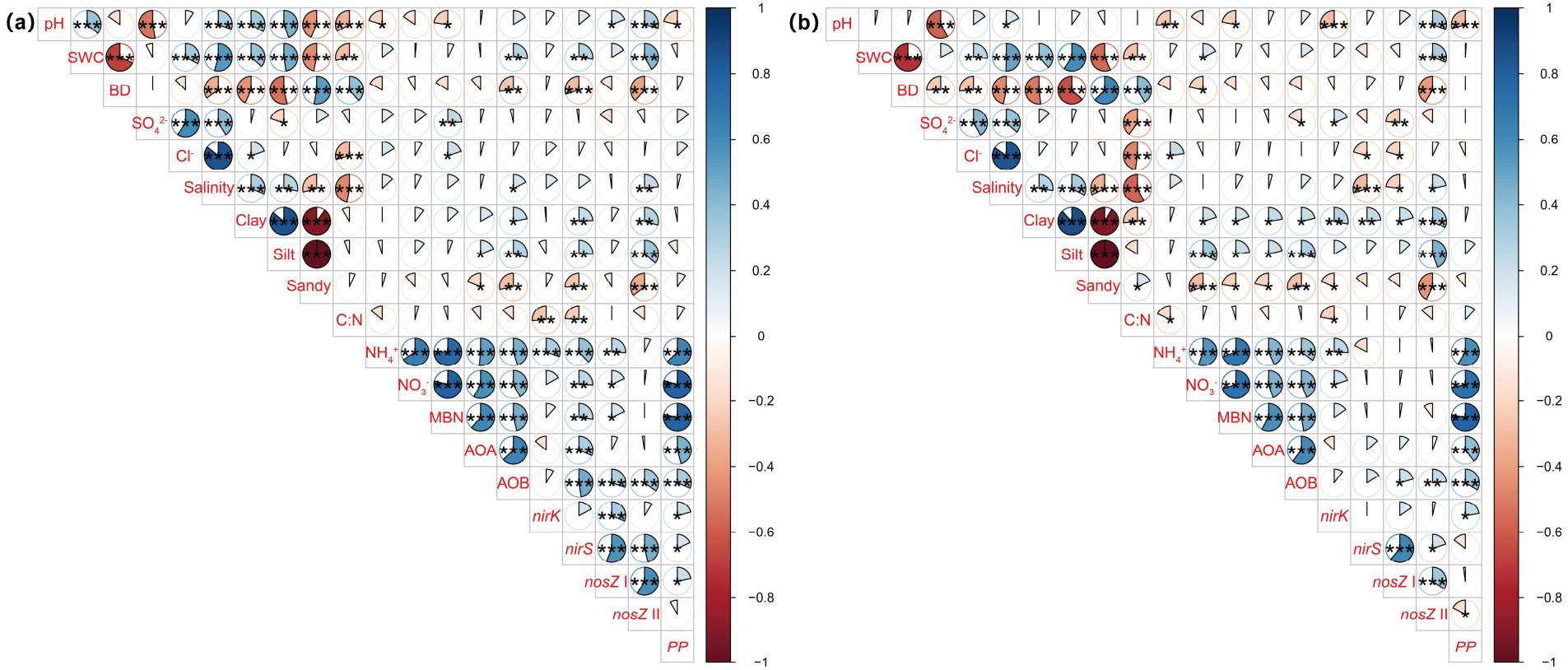

Figure 5. Correlations among environmental variables, abundances of nitrogen-cycling functional genes and sediment N_2O production potential (*PP*) (n = 216) for the different habitat modification scenarios: (a) conversion of mudflats to *S. alterniflora* marshes; (b) conversion of *S. alterniflora* marshes to aquaculture ponds. Color of the pie indicates the direction of correlation (blue = positive; red = negative). Size of the pie is proportional to the r^2 value. Asterisks indicate levels of significance (*$p < 0.05$; **$p < 0.01$; **$p < 0.001$).

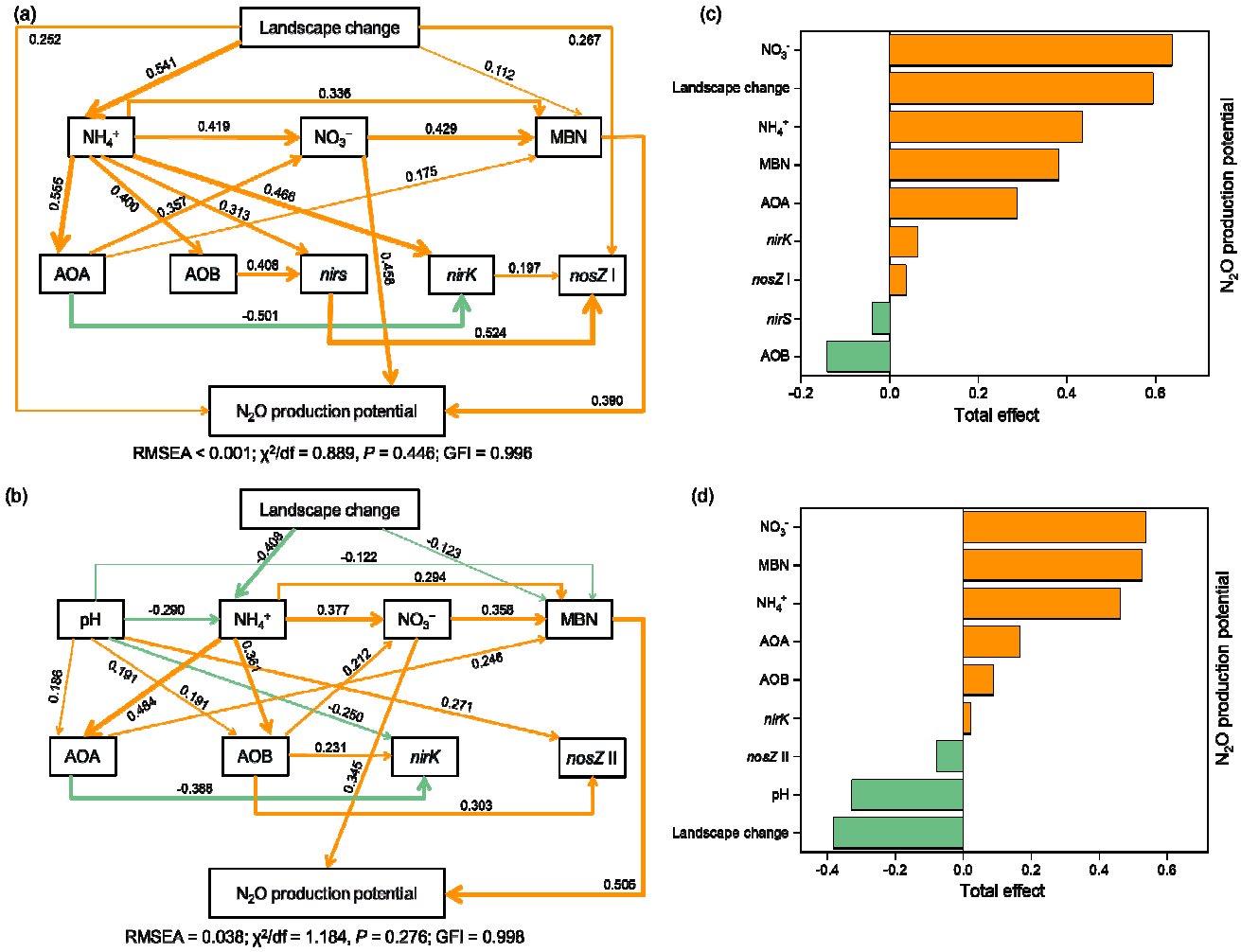

Figure 6. Structural equation models (SEM) to evaluate the direct and indirect effects of landscape change, sediment properties and the abundance of functional genes on N_2O production potential under different habitat modification scenarios: (a) conversion of mudflats to *S. alterniflora* marshes; (b) conversion of *S. alterniflora* marshes to aquaculture ponds. Total standardized effects of multiple factors on N_2O production potential for the respective habitat modification scenarios are shown in panel (c) and (d).

Supporting Information

Effects of landscape modification on coastal sediment nitrogen availability, microbial functional gene abundances and N_2O production potential across the tropical-subtropical gradient

Ping Yang[a,b,c,d*], Kam W. Tang[e], Linhai Zhang[a,b], Xiao Lin[a,b,c], Hong Yang[f,g], Chuan Tong[a,b,d*], Yan Hong[a], Lishan Tan[h], Derrick Y. F. Lai[h*], Yalan Tian[a], Wanyi Zhu[a], Manjing Ruan[a], Yongxin Lin[a,b,c*]

[a]*School of Geographical Sciences, Fujian Normal University, Fuzhou 350117, P.R. China*

[b]*Institute of Geography, Fujian Normal University, Fuzhou 350117, P.R. China*

[c]*Fujian Provincial Key Laboratory for Subtropical Resources and Environment, Fujian Normal University, Fuzhou 350117, P.R. China*

[d]*Key Laboratory of Humid Subtropical Eco-geographical Process of Ministry of Education, Fujian Normal University, Fuzhou 350117, P.R. China*

[e]*Department of Biosciences, Swansea University, Swansea SA2 8PP, U. K.*

[f]*College of Environmental Science and Engineering, Fujian Normal University, Fuzhou, 350007, China*

[g]*Department of Geography and Environmental Science, University of Reading, Reading, RG6 6AB, UK*

[h]*Department of Geography and Resource Management, The Chinese University of Hong Kong, Shatin, New Territories, Hong Kong SAR, China*

***Correspondence to:**

Ping Yang (yangping528@sina.cn); Chuan Tong (tongch@fjnu.edu.cn); Derrick Y. F. Lai (dyflai@cuhk.edu.hk); Yongxin Lin (yxlin@fjnu.edu.cn)

Telephone: 086-0591-87445659 **Fax:** 086-0591-83465397

Supporting Information Summary

No. of pages: 4 No. of figures: 0 No. of tables: 2

Page S3: TABLE S1 PCR primers and thermal cycling conditions used for gene quantification.

Page S4: TABLE S2 Surface soil physico-chemical properties across the three wetland habitat types. MFs, SAs and APs represent mud flats, *S. alterniflora* marshes and aquaculture ponds, respectively.

Table S1

PCR primers and thermal cycling conditions used for gene quantification.

Gene	Primer	Sequence	Thermal conditions	Reference
AOA *amoA*	Arch-*amoA*F	STAATGGTCTGGCTTAGACG	95°C, 3min；35×（95°C for 10 s, 55°C for 30 s, 72°C for 45 s+ plate read）；Melt curve：65.0°C to 95.0°C, increment 0.5°C, 0:05+ plate read	Francis et al., 2005
	Arch-*amoA*R	GCGGCCATCCATCTGTAT GT		
AOB *amoA*	amoA-1F	GGGGTTTCTACTGGTGGT	95°C, 3min；35×（95°C for 10 s, 55°C for 30 s, 72°C for 45 s+ plate read）；Melt curve：65.0°C to 95.0°C, increment 0.5°C, 0:05+ plate read	Rotthauwe et al., 1997
	amoA-2R	CCC CTC KGS AAA GCCTTCTTC		
nirS	nirSCd3aF	GTSAACGTSAAGGARACSGG	95°C, 3 min；35×（95°C for 10 s, 56 °C for 30 s, 72°C for 20 s+ plate read）；Melt curve：65.0°C to 95.0°C, increment 0.5°C, 0:05+ plate read	Throbäck et al., 2004
	nirSR3cd	GASTTCGGRTGSGTCTTGA		
nirK	nirKF1aCu	ATCATGGTSCTGCCGCG	95°C, 3 min；35×（95°C for 10 s, 56 °C for 30 s, 72°C for 20 s+ plate read）；Melt curve：65.0°C to 95.0°C, increment 0.5°C, 0:05+ plate read	Throbäck et al., 2004
	nirKR3Cu	GCCTCGATCAGRTTGTGGTT		
***nosZ* I**	nosZ1840F	CGCRACGGCAASAAGGTSMSSGT	95°C, 3 min；35×（95°C for 10 s, 58 °C for 25 s, 72°C for 20 s+ plate read）；Melt curve：65.0°C to 95.0°C, increment 0.5°C, 0:05+ plate read	Henry et al., 2006
	nosZ2090R	CAKRTGCAKSGCRTGGCAGAA		
***nosZ* II**	nosZ-II-F	CTIGGICCIYTKCAYAC	95°C, 3 min；35×（95°C for 10 s, 54 °C for 30 s, 72°C for 40 s+ plate read）；Melt curve：65.0°C to 95.0°C, increment 0.5°C, 0:05+ plate read	Jones et al., 2013
	nosZ-II-R	GCIGARCARAAITCBGTRC		

Table S2

Surface soil physico-chemical properties across the three wetland habitat types. MFs, SAs and APs represent mud flats, *S. alterniflora* marshes and aquaculture ponds, respectively.

Habitat	pH	Salinity (‰)	SWC (%)	SBD (g cm^{-3})	Cl^- (mg L^{-1})	SO_4^{2-} (mg L^{-1})	Soil particle size composition		
							Clay (%)	Silt (%)	Sandy (%)
MFs	7.99±0.06**a**	3.96±0.20**a**	43.05±1.33**b**	1.29±0.02**a**	36.84±2.15**b**	8.90±0.63**b**	10.41±0.47**a**	54.07±2.29**a**	35.53±2.69**b**
SAs	7.95±0.06**a**	4.54±0.23**a**	47.12±1.38**a**	1.26±0.02**a**	40.94±2.23**a**	9.13±0.50**b**	10.94±0.49**a**	52.67±2.41**bc**	36.38±2.86**b**
APs	7.82±0.06**a**	4.21±0.31**a**	47.78±1.70**a**	1.25±0.03**a**	37.75±3.43**b**	17.48±1.40**a**	10.50±0.57**a**	50.14±2.56**c**	39.35±3.06**a**

Lowercase letters within the same column indicate significant differences at $p < 0.05$ between three wetland habitat types. Data are after Yang et al. (2022) for reference and review only.

Reference

Yang, P., Zhang, L. H., Lai, D. Y. F., Yang, H., Tan, L. S., Luo, L. J., Tong, C., Hong, Y., Zhu, W. Y., Tang, K. W., 2022. Landscape change affects soil organic carbon mineralization and greenhouse gas production in coastal wetlands. *Global Biogeochemical Cycles*, *36*, e2022GB007469. https://doi.org/10.1029/2022GB007469